Journal of Applied Polymer Science

Melt extrusion of polyethylene nanocomposites reinforced with nanofibrillated cellulose from cotton and wood sources

Nasim Farahbakhsh,[1] Peiman Shahbeigi Roodposhti,[2] Ali Ayoub,[3] Richard A. Venditti,[3] Jesse S. Jur[1]

[1]Department of Textile Engineering, Chemistry and Science, North Carolina State University, Raleigh, North Carolina 27695
[2]Department of Materials Science and Engineering, North Carolina State University, Raleigh, North Carolina 27695
[3]Department of Forest Biomaterials, North Carolina State University, Raleigh, North Carolina 27695
Correspondence to: J. S. Jur (E-mail: jsjur@ncsu.edu)

ABSTRACT: Replacing petroleum-based materials with biodegradable materials that offer low environmental impact and safety risk is of increasing importance in sustainable materials processing. The objective of this study was to produce uniform nanofibrillated cotton from recycled waste cotton T-shirts using microgrinding techniques and compare its performance as reinforcing agent in thermoplastic polymers constructs with wood-originated materials. The effect of the microgrinding process on morphology, crystallinity, and thermal stability of materials was evaluated by transmission electron microscopy (TEM), scanning electron microscope (SEM), X-ray diffraction (XRD), and thermogravimetry analysis (TGA). Nanofibrillated cotton resulted in higher crystallinity and thermal stability than fibrillated bleached and unbleached softwood. All the materials were extruded with low-density polyethylene to fabricate nanocomposite films. Nanofibrillated cotton nanocomposites had a higher optical transparency than did the wood-based composites. The mechanical properties of the nanofibrillated cotton nanocomposites were largely improved and showed 62.5% increase in strength over the wood-based nanofibrillated containing composites, in agreement with the higher crystallinity of the nanosized cotton-derived filler material. © 2015 Wiley Periodicals, Inc. J. Appl. Polym. Sci. **2015**, *132*, 41857.

KEYWORDS: biomaterials; extrusion; structure; property relations

Received 27 July 2014; accepted 25 November 2014
DOI: 10.1002/app.41857

INTRODUCTION

Cellulose, the most abundant natural polymer, has gained prominence for the fabrication of nanoscale materials in two major forms of crystalline nanocellulose (CNC) and nanofibrillated/microfibrillated cellulose (NFC/MFC).[1] These nanosized cellulose fibers are of high interest in the fields of nanotechnology and nanocomposites due to their abundance, nontoxicity, biodegradability, low weight, and high strength and stiffness per unit of weight.[1]

Cellulose originates from various natural sources, including wood, plant (such as cotton, sisal, flax, jute, and ramie.), algae, bacterial cellulose, and tunicate cellulose. While over the last two decades, pulp-based cellulose has attracted the majority of attention as a reinforcing agent in developing new polymer nanocomposites, nanocellulose derived from cotton offers advantages due to its high cellulose content that results in high yield without any intensive purification process.[2] Cotton is the most commercially important seed fiber, and cotton fibers have been used in the textile industry for garments and furniture for more than 1000 years due to its excellent properties.

Cotton is a convoluted fiber that consists of about 95% cellulose and includes cuticle, primary wall, secondary wall and a central canal called lumen. A ribbon-like cotton fiber is 65–85% crystalline with a length of 1.2–5 cm and diameter of 15–20 μm. In wood pulp, cellulose microfibrils and hemicellulose are present in all of the fiber's regions, including the middle lamella, primary wall, and the secondary wall. The wood fiber is a composite of cellulose nanofibers embedded in a gel-like matrix of lignin, hemicellulose, and extractives. Cellulose percentage depends on wood types and species and a typical distribution of cellulose, lignin, hemicellulose, and extractives for softwood is 42%, 27%, 28%, and 3%, respectively.[3]

Nanofibrillated cellulose (NFC) from purified cellulose of wood pulp was first isolated in 1983 by Turbak *et al.* using high-pressure homogenizer to produce long and flexible agglomerates of cellulose nanofibrils of < 100 nm diameter and lengths of several micrometers.[4,5] Stable aqueous suspension of NFC has found multiple applications in painting, coating, cosmetics, medical, and food industry as thickener and emulsifier. Typically, NFC is obtained through the following three mechanical

methods: high-pressure homogenizer, microfluidizer, and micro-grinding.[6] NFC can be isolated from simple mechanical treatment or a combination of chemical pretreatment and mechanical methods. Studies on NFC characteristics and energy consumption of these methods showed that NFC material achieved through the use of a microgrinder requires a lower total energy input.[7] NFC is characterized as a highly porous structure with a large surface to volume ratio and a low coefficient of thermal expansion (10^{-7} K^{-1}).[8] As a result, NFC has also demonstrated application in reinforced materials, filtration, and scaffold tissue engineering.[6]

Our previous study investigated the possibility of fabrication of nanofibrillated cotton through microgrinding and studied the effect of cotton fiber size and polymer shape (pellets vs. powder) on physical properties of thermoplastic polymer composites.[9] The goal of this work is to compare morphological and crystallinity differences in NFC material originating from bleached softwood, unbleached softwood, and cotton. Using this analysis, the structure/property relationships with respect to the reinforcing capability of NFC from the three sources will be investigated through mechanical testing of low-density polyethylene (LDPE) nanocomposite films.

EXPERIMENTAL

Materials

Pulverized cotton with (pCot) with an average fiber length of 350 μm was acquired from the International Fiber Corporation (derived from recycled T-shirts). Unbleached and bleached softwood (UBSW and BSW) pine Kraft pulp samples were obtained from kraft pulp mills in the Southeast United States. LDPE was acquired from Dow Chemical Company (PN: ASPUN™ 6850 A) with density of 0.955 g.cm^{-3} and melt flow index of 30 g per 10 min.

Nanofibrillated Cellulose Preparation

NFC using pulverized cotton (NFC-pCot), bleached softwood (NFC-BSW), and unbleached softwood (NFC-UBSW) were prepared individually from an aqueous suspension of each material with 3 wt % solid consistency by sequentially passing the suspension through a 10-inch Masuko Super MassColloider (Masuko Sangyo Co., Kawaguchi-city, Japan) at 1500 rpm for a total of nine passes. Before microgrinding, the bleached and unbleached pulps were refined by dispersing the pulp in water with 3 wt % consistency using a laboratory-scale Valley Beater (Valley Iron Works, Appleton, WI) for a total refining time of 2 h and stored in a cold room until needed. After the microfibrillation, the suspension was freeze-dried at −50°C using a Labconco Freeze Dryer.

Fabrication of Nanocomposite Films

Nanocomposite materials were prepared by melt extrusion of low-density polyethylene as resin polymer in powder form with 2.5, 5, and 10 wt % of each NFC materials individually as reinforcing filler using a twin-screw extruder extruder (Xplore, Micro 15cc Twin Screw Compounder) at 170°C, 10 min, and 50 rpm. Polymer powder was prepared using a Freezer Mill at frequency of 10 Hz and 7 cycles using liquid nitrogen. For tensile testing, nanocomposite films were fabricated from the extruded material in a standard dog-bone shape (60 × 60 × 0.24 mm^3) using a hot press at 170°C under a force of 3500 psi.

Characterization of NFCs and Composites

The morphology of NFC-pCot, NFC-BSW, and NFC-UBSW after nine passes of microgrinding was investigated by transmission electron microscopy (TEM) JEM-2000FX. TEM samples were prepared by placing a single droplet of diluted NFC suspension onto a copper grid covered with a carbon film and dried. The effect of microgrinding process on the morphology of NFC-pCot, NFC-BSW, and NFC-UBSW after 2, 4, and 9 microgrinding passes was investigated using a Phenom, G2 Pro scanning electron microscope (SEM). SEM samples were prepared by freezing of aqueous suspension of each material with 0.1 wt % consistency at liquid nitrogen and drying the samples using freeze dryer. The relative degree of crystallinity (X_c%) or crystallinity index (CrI) of NFC materials with an increasing number of mechanical passes of microgrinding was determined using an Omni Instrumental X-ray diffractometer. The diffractometer is equipped with Be-filtered Cu–Kα radiation with a wavelength of 1.54 Å generated at 35 kV and 25 mA. The samples were scanned from a 2θ range from 5 to 45° at an increment of 0.05°. Relative degree of crystallinity was calculated from the intensity measurements using the Segal method,

$$X_c\% = \left(\frac{I_{002} - I_{AM}}{I_{002}}\right) \times 100 \quad (1)$$

in which I_{002} represents the maximum intensity of (002) lattice diffraction peak at diffraction angle around 2θ=22.5° and I_{AM} represents the intensity scattered by the amorphous component in the sample, which was evaluated as the lowest intensity at 2θ of 18°.[10,11]

The optical properties of LDPE nanocomposite films were investigated using a Varian Cary 300 UV-Visible spectrometer in wavelength range of 200–700 nm. Tensile tests were performed using a Q-test tensile tester with 250 lb load cell and 60 mm gage length according to ASTM D 882. Experiments were performed at room temperature on dog-bone shape samples at a crosshead speed of 10 mm min^{-1}. The reported values for each sample were determined from the average of at least five measurements. The microstructure of pure polymer and LDPE nanocomposite films at their fracture point obtained using liquid nitrogen was observed by scanning electron microscopy using a Verios 460L SEM scanning electron microscope. Finally, thermal degradation analysis of the reinforcing agents and composite samples was carried out using a Perkin-Elmer thermo gravimetric analyzer (TGA) at a heating rate of 10°C min^{-1} from 25 to 600°C in a nitrogen atmosphere. The thermal characterization of the LDPE nanocomposites was analyzed using Perkin-Elmer differential scanning calorimeter (DSC). The samples were heated from 25 to 160°C and allowed to stand for 5 min at 160°C and then cooled from 160 to 25°C under nitrogen atmosphere with the heating/cooling rate at 10°Cmin^{-1}. The melting and the crystallization temperatures were obtained using heating and cooling cycles, respectively. The degree of crystallinity of the nanocomposites (X_c%) was calculated using the following eq. (2):

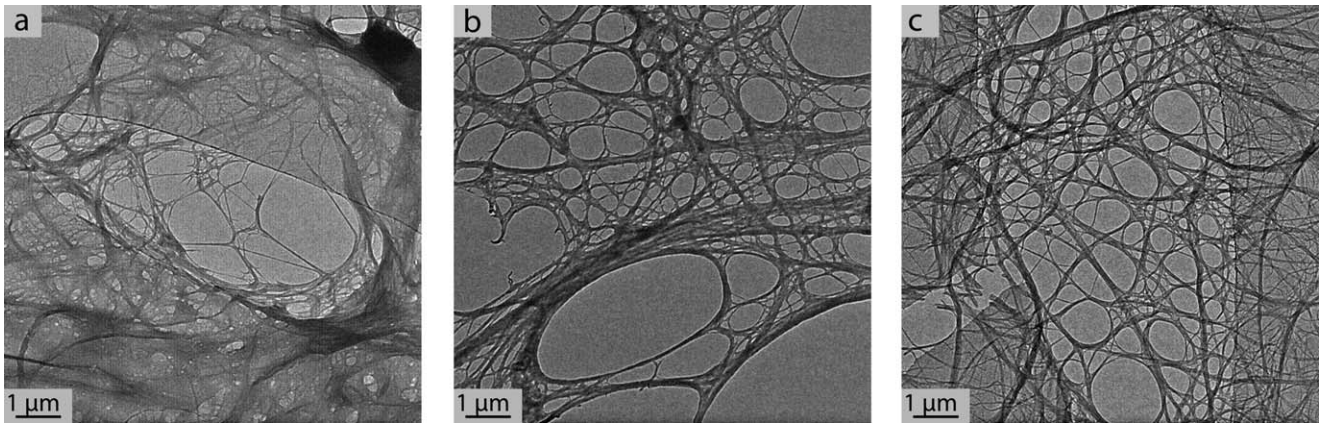

Figure 1. TEM images of NFC-pCot (a), NFC-UBSW (b) and NFC-BSW (c) after 9 passes of the microgrinding process.

$$X_c\% = \left({}^{\Delta H_m}/_{w.\Delta H_m^*} \right) \times 100 \quad (2)$$

Where ΔH_m is the enthalpy of fusion/crystallization (Jg^{-1}), w the weight fraction of LDPE matrix in the nanocomposites and ΔH_m^* is the heat of fusion of completely crystalline LDPE polymer ($\sim 287\ Jg^{-1}$).[12,13]

RESULTS AND DISCUSSION

Characterization of NFCs

TEM analysis of a dilute suspension of nanofibrillated cellulose from cotton, unbleached, and bleached softwood sources after nine microgrinder passes are provided in Figure 1. The morphology of NFC samples reveals a network of nanofibrillated fibers with fibril diameters of 10–100 nm and a length of several microns that are aggregated due to high number of hydrogen bonding between nanofibrils. Figure 2 compares the SEM images of freeze-dried NFC from three different sources and shows the effect of increasing number of passes on the microgrinding process from 2 to 9 passes. Freeze drying of NFC suspension after mechanical treatment causes formation of additional -OH bonds between amorphous parts of cellulosic fibrils resulting irreversible aggregation of fibril bundles together known as hornification of NFC (irreversible aggregation of fibril bundles).[14] As indicated in the images, increasing the number of passes gradually enhances fibrillation of fibers. At two passes, cotton fibers are more fibrillated compared to bleached and unbleached softwood originated fibers. For any number of passes of microgrinding, the NFC-pCot revealed smaller elements as compared to bleached and unbleached softwood fibers.

Due to the high mechanical force applied by the microgrinding process, the crystallinity of the cellulose is expected to be altered. Figure 3 shows X-ray diffraction (XRD) patterns of NFC from three cellulose sources before and after nine passes of microgrinding process. Nanofibrillated cotton, maintained the native crystalline structure of cellulose Type I with the main characteristics peaks of native cellulose at 2θ of 15°, 16°, 22.5°, and 34° that is attributed to diffraction planes of $101, 10\bar{1}, 002,$ and 040. [11] Table I also presents the calculated crystallinity index or relative degree of cellulose crystallinity ($X_c\%$) of NFC-pCot, NFC-UBSW, and NFC-BSW after 0, 2, 4, 7, and 9 microgrinding passes using Segal method, and the NFC-pCot displays the highest crystallinity after microgrinding process. It should be noted that different calculation methods affect the reported cellulose crystallinities because of the overlapping and widely broadened diffraction peaks of cellulose. The Segal method generally results in the highest crystallinity values compared to other calculations.[10,11,15] With increasing number of microgrinding passes, the relative degree of crystallinity decreases for all materials but remains higher for nanofibrillated cotton. Homogenization processing of NFC extracted from softwood and hardwood by Spence *et al.* has shown a similar reduction in the crystallinity of cellulose nanofibers and was attributed to the fiber structure degradation during mechanical treatment. In addition, an increase in the number density of crystals at the surface of the fibrils is predicted that results in disorganized lateral cohesion and no periodic lateral hydrogen bonds that contribute to the amorphous parts.[16] It is expected that the bleached softwood would show increased crystallinity relative to the unbleached softwood as the bleaching process removes lignin and hemicellulose, branched compounds that do not pack effectively and are noncrystalline. Iwamoto *et al.* calculated the degree of crystallinity of pulp fibers as an indicator of fiber degradation through microgrinding process.[17] The degree of crystallinity, defined as the percentage of the area of crystalline reflection to the whole area of the scattering profile, decreased from 60% to 40% after 10 microgrinding passes.[17] Abe *et al.* showed that the first grinding pass of cellulosic from different sources increased the relative degree of crystallinity from 71% to 78.6% for wood fibers, from 68.2% to 76% for rice straw, and from 66.1% to 80.2% for potato tuber since the amorphous parts are more susceptible to shear forces than the crystalline region and disintegration of fibers occurs in amorphous parts first.[18] Cheng *et al.* obtained similar results for lyocell fibers using ultrasonication and the relative degree of crystallinity improved from 61.2% to 75.8% after 20 min.[11]

Thermal degradation behavior of cellulosic reinforcing agents was evaluated using TGA measurements. A summary of the results are provided in Figure 4 and Table II. All the cellulosic reinforcing agents have a small weight loss from room temperature to 100°C due to the evaporation of water. Thermal stability

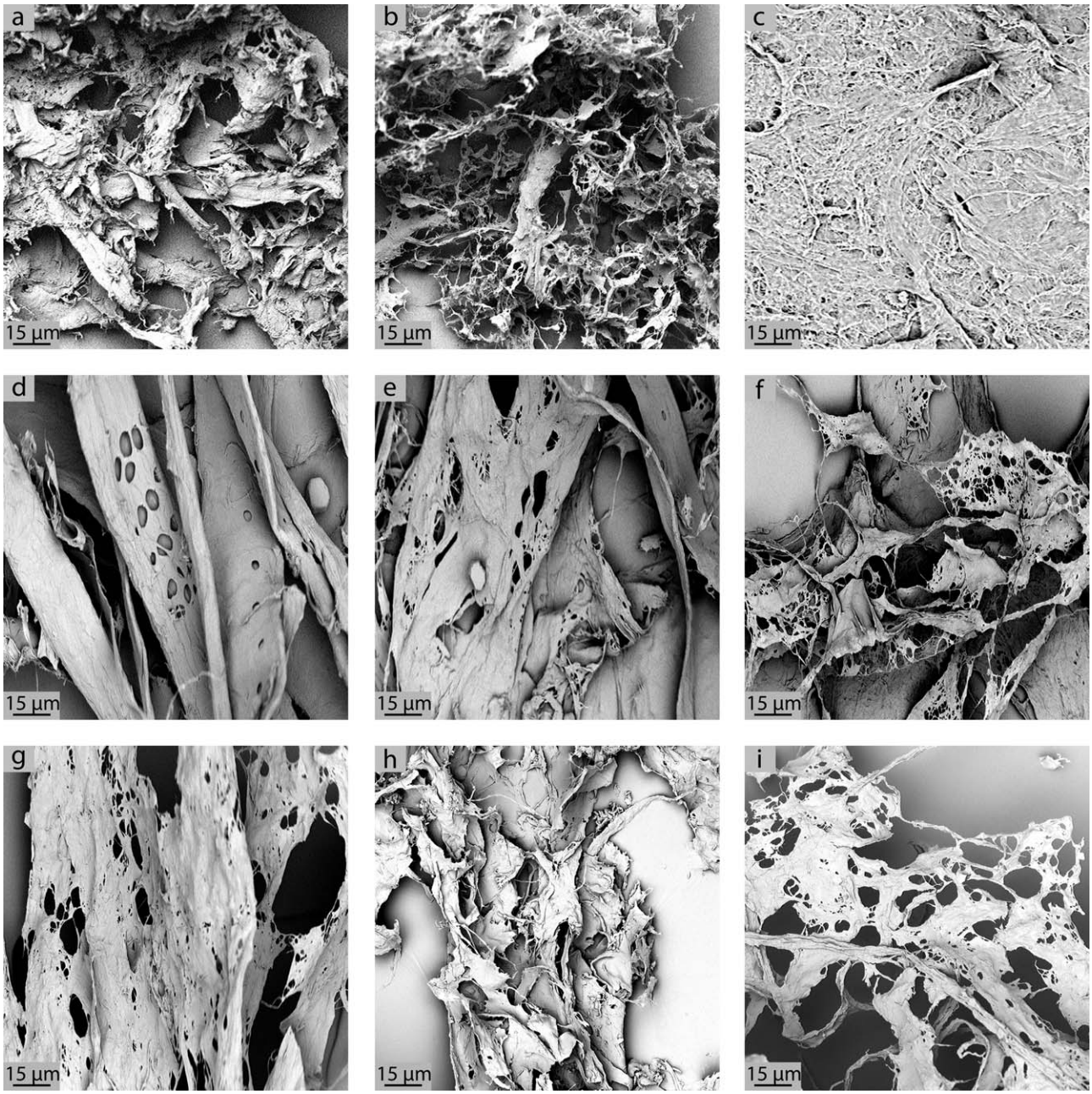

Figure 2. SEM images of freeze dried NFC-pCot (a-c), NFC-BSW (d-f), and NFC-UBSW (g-i) after 2 (a,d,g), 4 (b,e,h), and 9 (c,f,i) microgrinding passes.

analysis of NFC from Daicel Chemical Industries also revealed an initial weight loss less than 100°C due to moisture content of NFC and decomposition temperature of 365°C.[19] The values of T_{onset} (the beginning of the degradation process) and T_d (maximum rate of degradation temperature) correspond to the intersection of two tangents in the mass versus temperature data and the minimum of the derivative of TGA signal, respectively. As the plot shows, NFC-pCot shows a higher thermal stability compared to the wood based cellulose fillers with T_{onset} at 336.2°C and T_d at 374.1°C. NFC-BSW revealed the lowest thermal stability with T_{onset} of 295°C and the maximum degradation temperature (T_d) of 333.2°C. Lu *et al.* reported similar values for NFC from kraft wood pulp with the onset thermal degradation of NFC at 280°C and the maximum degradation temperature at 350°C.[20] Tingaut *et al.* reported the onset temperature of 290°C for homogenized bleached sulfite wood pulp at 5% weight loss.[6]

Nanocomposite Characterization

To compare the reinforcing capabilities of the nanofibrillated cellulose materials, LDPE nanocomposites reinforced with NFC-pCot, NFC-BSW, and NFC-UBSW reinforcing agents were characterized in terms of reinforcing filler dispersion, thermal degradation, and mechanical properties. Based on previous results of

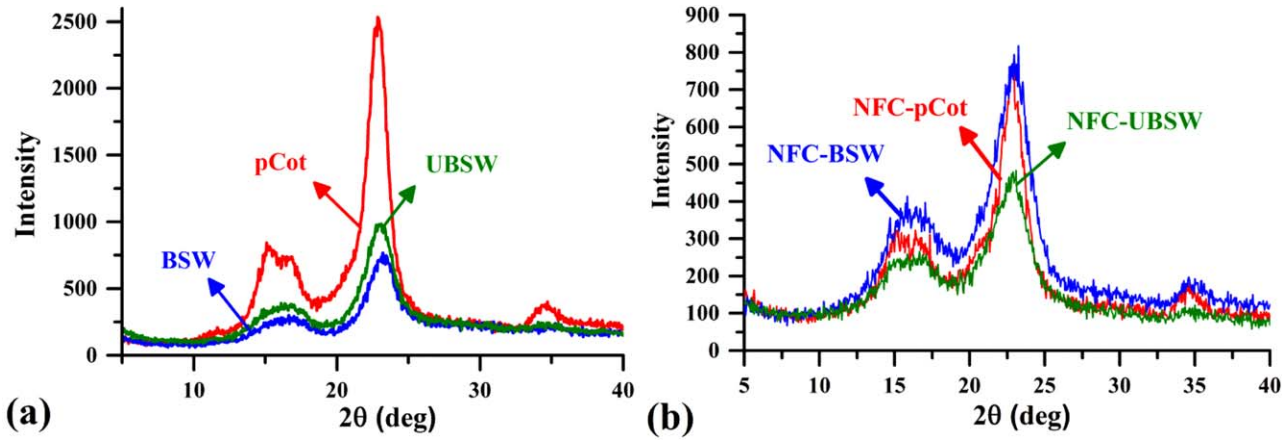

Figure 3. X-ray diffraction patterns for (a) pCot, BSW, and UBSW before microgirnding and (b) NFC-pCot, NFC-BSW, and NFC-UBSW after nine passes of the microgrinding process. [Color figure can be viewed in the online issue, which is available at wileyonlinelibrary.com.]

obtaining improved filler distribution and increased mechanical properties of NFC-pCot/LDPE nanocomposite films with LDPE powder rather than LDPE pellets, all the fillers were compounded with LDPE powder.[9] The optical properties of NFC-reinforced LDPE nanocomposites were investigated by visual inspection and by using a UV-Vis spectrometer to determine the transmittance of light through the nanocomposite films. The quality of reinforcing agent distribution in the polymer matrix and changing the color of Figure 5 provides visual inspection of the LDPE and the LDPE nanocomposite films with an average thickness of 0.25 mm for up to 10 wt % NFC reinforcement. Comparing to neat LDPE film, nanocomposite sheets are less translucent and aggregated NFC appeared as white dots throughout the films. As compared to NFC-pCot, wood-based reinforcing agents show less uniform distribution and larger white dots due to aggregation of reinforcing filler in the polymer matrix. Moreover, the presence of wood-based NFCs caused a change in color of the LDPE nanocomposite and was more pronounced with an unbleached softwood and increasing reinforcing agent content. In contrast, the NFC-pCot nanocomposites had no discoloration. It is important to note that there is no discoloration or evidence of degraded NFC in the composite films after 10 min of melt extrusion at 170°C (through an internal recirculation within the extruder) regardless of reinforcing agent type.

Figure 6 compares the differences in the light transmittance of nanocomposite sheets including 2.5 and 10 wt % NFC reinforcing agents with pure polymer film. In general, nanocomposite films suffer from loss of transparency due to increased light scattering. Optically transparent nanocomposites could be obtained using reinforcing agents with smaller size and more uniform distribution within the matrix. Overall, the NFC-pCot nanocomposite films revealed a higher transparency compared to wood-based nanocomposites. Addition of reinforcing agent from 2.5% to 10 wt % reduced the transparency of materials about two times regardless of reinforcing agent type. At a wavelength of 600 nm, the middle of the visible wavelength range, the light transmittance (*T*%) of 10 wt % NFC-pCot is only 7% lower than LDPE film, while *T*% NFC-UBSW is reduced by 17%. The difference among the films is more pronounced at lower wavelength and at 400 nm, *T*% is 25%, 29%, and 70% lower than the light transmittance of pure polymer for 10 wt % of NFC-pCot, NFC-BSW, and NFC-UBWS nanocomposite films, respectively.

The effect of the type of reinforcing filler on the elastic modulus, tensile strength, and elongation at break of LDPE nanocomposites with loading amounts of 2.5, 5, and 10 wt % is shown

Table I. Relative Degree of Cellulose Crystallinity (X_c%) or Crystallinity index (CrI) of NFC-pCot, NFC-BSW, and NFC-UBSW after 2, 4, 7, and 9 Microgrinding Passes Using Segal Method

Grinding passes	NFC-pCot	NFC-BSW	NFC-UBSW
0	86.1	81.2	79.5
2	83.6	80.5	74.0
4	79.5	79.4	71.6
7	77.5	71.7	69.6
9	77	71.3	69.1

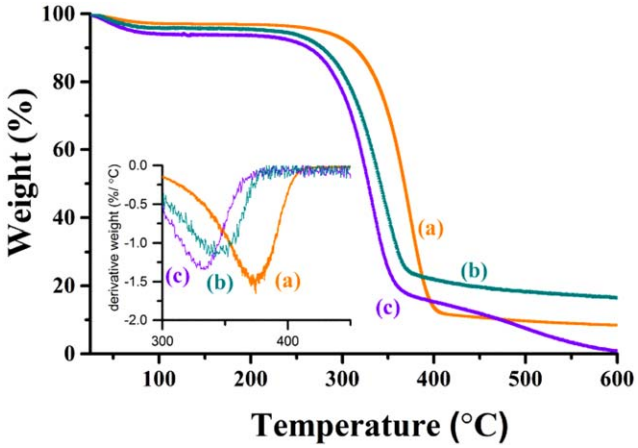

Figure 4. Thermogravimetric (TG) curves and derivative TG showing weight % and derivative of weight (%/°C) over temperature of (a) NFC-pCot, (b) NFC-UBSW, and (c) NFC-BSW. [Color figure can be viewed in the online issue, which is available at wileyonlinelibrary.com.]

Table II. Summary of d-TGA Analysis of NFC-pCot, NFC-BSW, and NFC-UBSW

Sample	T_{onset} (°C)	T_d max. (°C)
NFC-pCot	336.2 ± 2.3	374.1 ± 2.6
NFC-BSW	295 ± 4.1	333.2 ± 2.4
NFC-UBSW	304.3 ± 4.5	347.4 ± 4.4

in Figure 7. The elastic modulus and tensile strength of reinforced nanocomposites using 10 wt % NFC-pCot/LDPE was 80% greater than LDPE polymer while 10 wt % of wood-based reinforcing agents only improved the elasticity of NFC-BSW/LDPE and NFC-UBSW/LDPE by ~15% [Figure 7(a)]. Interestingly, the NFC-pCot reinforced LDPE nanocomposites showed an approximately constant tensile strength with wt %, whereas the wood-based fillers showed decreased tensile strength [Figure 7(b)]. A uniform filler distribution within a polymer matrix results in a better stress transfer properties between filler and polymer. The 5 and 10 wt % of NFC-pCot-reinforced LDPE nanocomposites showed an increased elongation at break by a factor of ~1.5x compared to wood-based fillers [Figure 7(c)]. It is of interest to note that the bleached and unbleached softwood-based fillers behave very similarly. This has important implications since the unbleached fibers have a higher manufacturing yield and less processing steps that decrease their cost, complexity of manufacturing and environmental burden relative to bleached fibers. The results of tensile testing measurement by Seydibeyoglu using homogenized hardwood NFC-reinforcing polyurethane matrix also improved the elastic modulus and tensile strength of nanocomposite drastically due to small size of NFC particles and interaction between polymer and a reinforcing agent.[21] Incorporation of acid-treated NFC from cotton (Whatman filter paper) and softwood also improved the mechanical properties of thermoplastic extruded starch matrix.[8] Similar improvement in mechanical properties of amylopectin nanocomposite film was obtained using mechanically treated (with microfluidizer) NFC from enzyme-treated bleached sulfite softwood pulp due to reinforcing capability of entangled nanofibers.[5]

To understand this behavior in more detail, Figure 8 provides SEM imaging of pure polymer and LDPE with 10 wt % of each filler type at the fracture point (under liquid nitrogen) to evaluate the interaction between polymer matrix and each filler. SEM image of pure polymer reveals a smooth surface and a brittle fracture compared to the NFC-compounded polymer nanocomposites. SEM imaging of NFC-pCot nanocomposite reveals a network of nanofibers inducing more plastic deformation that absorbs more energy due to better adhesion and stronger interactions between polymer and the NFC-pCot-reinforcing agent compared to the softwood fillers. The images are consistent with higher toughness of LDPE nanocomposites compounded with NFC-pCot.

Thermal behavior of nanocomposites at different contents of reinforcing agent and the neat polymer is summarized in Table III, and the results for 10 wt % filler are plotted in Figure 9. The composites show a weight loss in the range of 300–400°C corresponding to the degradation of the cellulose. The onset

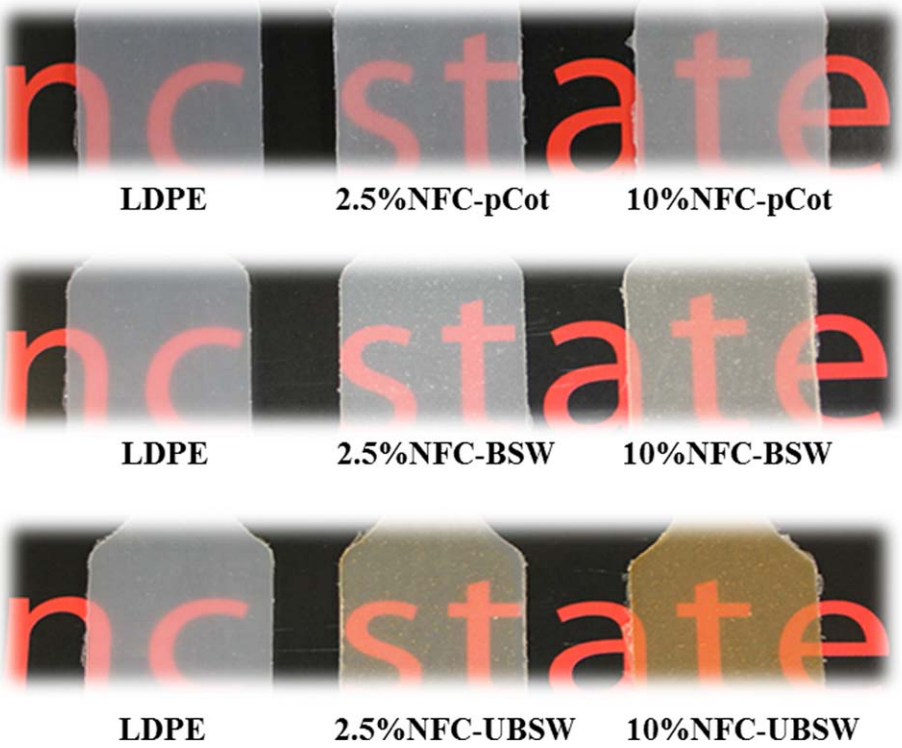

Figure 5. Optical micrographs of LDPE nanocomposite films with pure LDPE powder, and 2.5, 10 wt % NFC-pCot-, NFC-BSW-, and NFC-UBSW-reinforcing agents respectively. [Color figure can be viewed in the online issue, which is available at wileyonlinelibrary.com.]

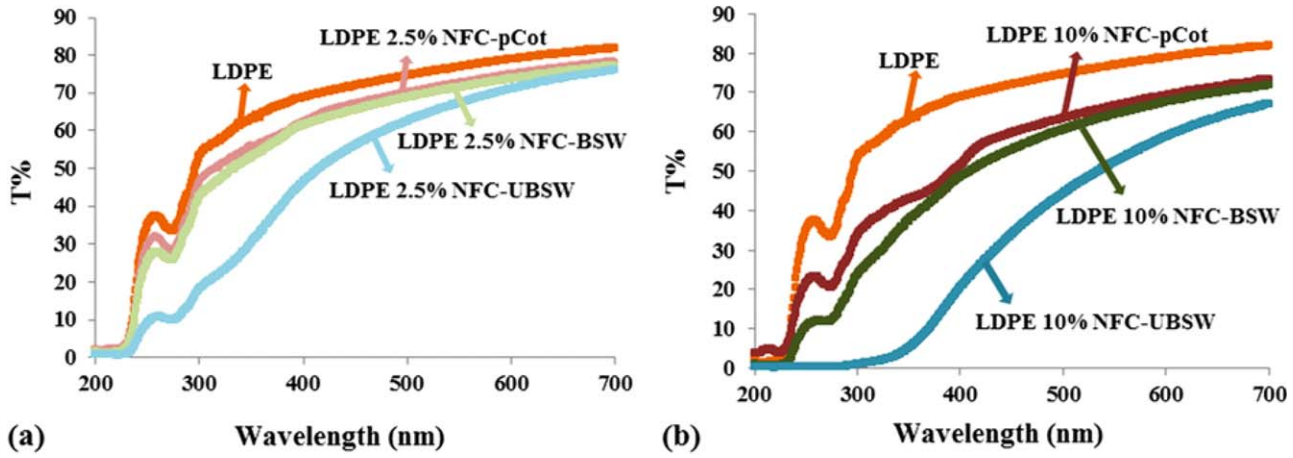

Figure 6. Light transmittance of LDPE nanocomposite films with (a) 2.5 wt % and (b) 10 wt % reinforcing agents using UV-Vis instrument. [Color figure can be viewed in the online issue, which is available at wileyonlinelibrary.com.]

temperature is related to degradation of cellulosic filler as observed in thermal analysis of reinforcing agents (Table II). As compared to the NFC softwood containing composites, the NFC-pCot nanocomposite reveals a higher onset temperature due to higher thermal stability of NFC-pCot (Figure 4) as expected. Interestingly, the degradation of the LDPE, as reported as T_d is increased for all filler sources at almost all filler levels. This increase in T_d may be due to interaction between thermal degraded products of polymer and reinforcing filler that could stabilize and protect the nanocomposite at high

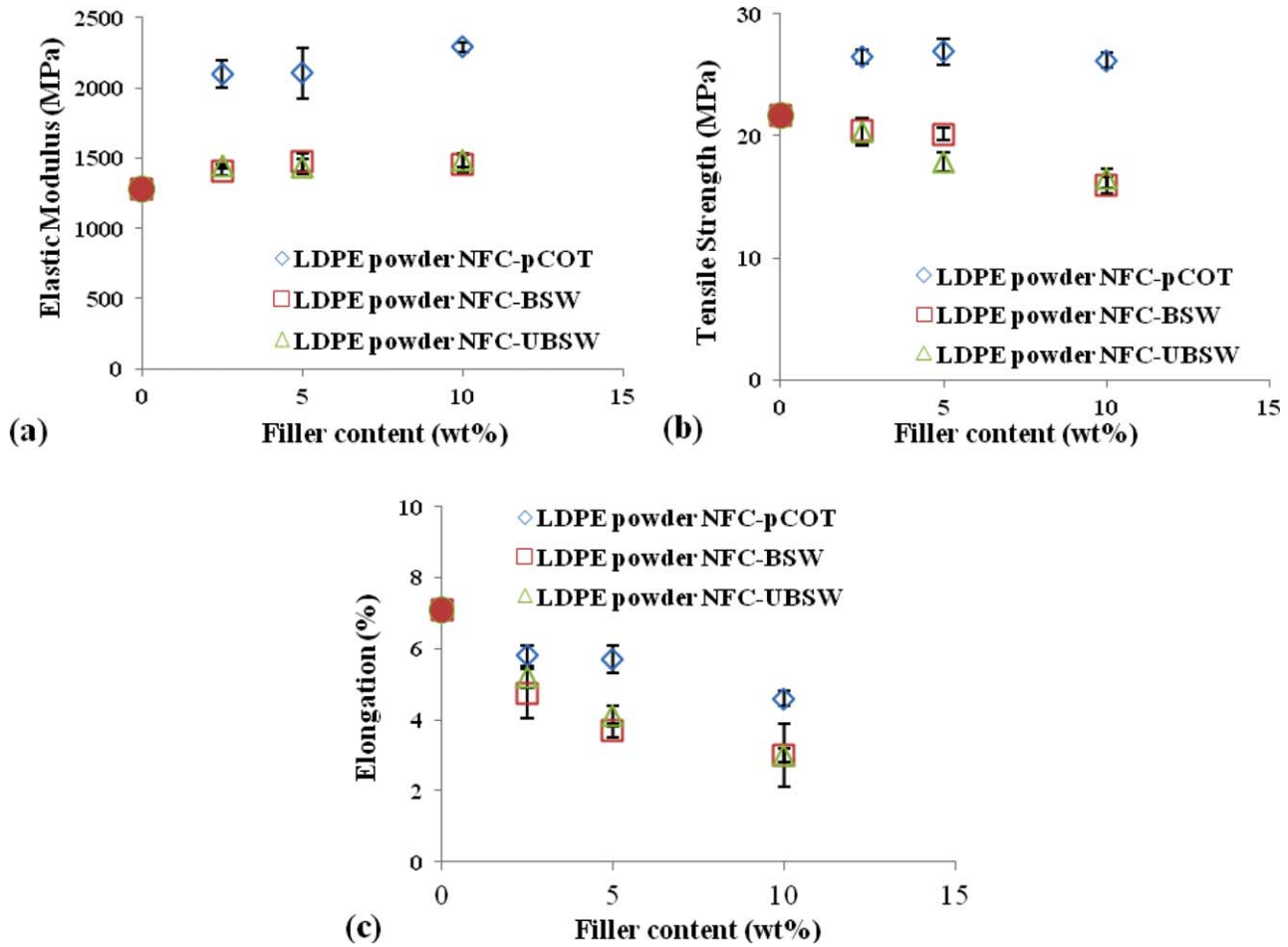

Figure 7. Mechanical properties of LDPE powder with NFC-pCot, NFC-BSW, and NFC-UBSW at filler content of 2.5%, 5%, and 10 wt %. [Color figure can be viewed in the online issue, which is available at wileyonlinelibrary.com.]

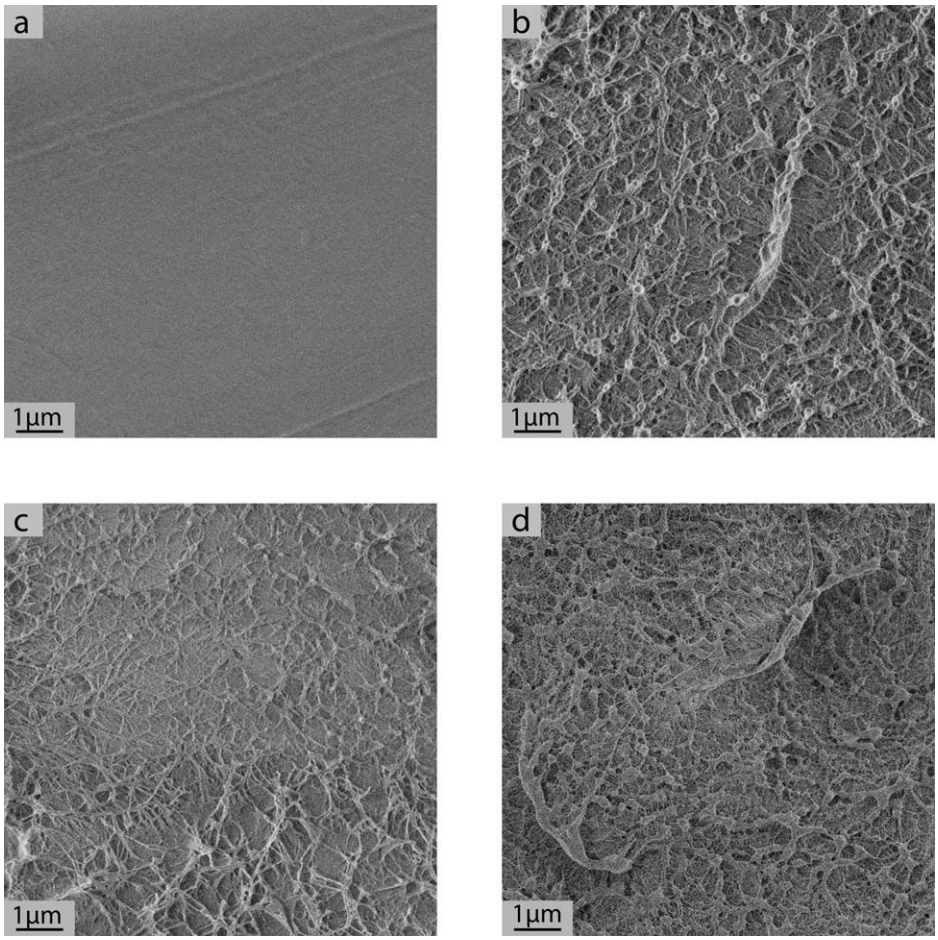

Figure 8. SEM images of the fracture point of (a) pure LDPE and composite films of LDPE with 10 wt % of (b) NFC-pCot, (c) NFC-BSW, and (d)NFC-UBSW, respectively.

temperature. Aggregation of fillers reduces onset temperature of polymer nanocomposites, while van der Waals interactions with polymer host enhance the thermal stability.[22]

Analysis of DSC traces of the heat flow rate over a temperature determines melting temperature, crystallization temperature, and heat of fusion/crystallization of pure polymer- and NFC-reinforced LDPE nanocomposites. The thermograms and resulting experimental data are reported in Figure 10 and Table IV. The melting point (T_m) of LDPE nanocomposites up to 10 wt % of reinforcing agent remained constant for NFC-pCot samples and caused only a marginal effect (~2°C) for wood-based LDPE nanocomposites. The reinforcing agents do not interfere with the crystal growth of LDPE polymer regardless of their type. Literature results indicate little to no variation of the melting temperature for most cellulose nanocrystalline nanocomposites. Menezes *et al.* reported a similar behavior for cellulose whiskers reinforced LDPE nanocomposites indicating that ramie cellulose nanowhiskers had no effect on the size of crystallites.[12] In contrast, NFC from wheat straw fibers reinforced thermoplastic starch reduced the melting temperature of nanocomposite from 118.67°C for neat polymer to 98.57°C with 15% NFC due to restriction of crystal growth.[23]

Table III. Degradation Data of LDPE Powder with NFC-pCot, NFC-UBSW, and NFC-BSW at Different Filler Content

Sample	T_{onset}	T_d (°C)
LDPE	NA	482.5 ± 3.9
LDPE 2.5% NFC-pCot	325.1 ± 6.7	487.7 ± 0.4
LDPE 5% NFC-pCot	321.1 ± 2.0	496 ± 7.8
LDPE 10% NFC-pCot	326.6 ± 7.3	500 ± 4.9
LDPE 2.5% NFC-BSW	321.8 ± 7.8	497.2 ± 4.8
LDPE 5% NFC-BSW	320.4 ± 9.2	498 ± 5.2
LDPE 10% NFC-BSW	310.2 ± 5.7	502.5 ± 4.8
LDPE 2.5% NFC-UBSW	319.1 ± 2.2	497.7 ± 3.2
LDPE 5% NFC-UBSW	310.7 ± 0.6	498.1 ± 4.3
LDPE 10% NFC-UBSW	310.1 ± 8.3	498.5 ± 0.5

The crystallization temperature (T_c) is obtained from the cooling cycle and is roughly constant regardless of reinforcing agent type and content in the polymer matrix (Table IV). T_c is directly correlated with facile organization of polymer chains and formation of crystal domains. The literature reported higher crystallization temperature in the presence of compatiblizer. Siqueira *et al.* reported a 10°C increase in T_c for polycaprolactone polymer reinforced with modified cellulose nanowhisker and modified NFC from sisal fibers.[24] Similar results obtained for 20% NFC

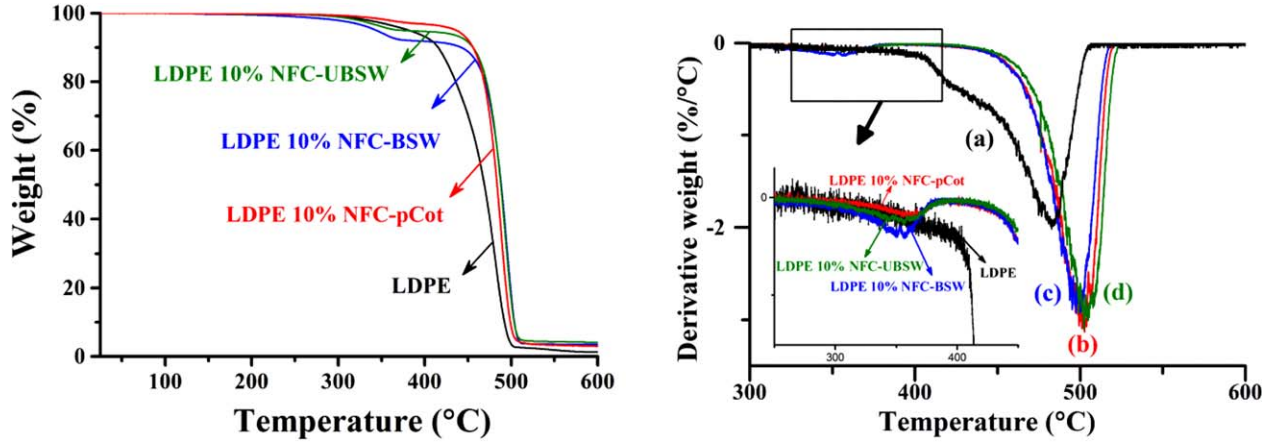

Figure 9. (left) Thermogravimetric (TG) curves and (right) derivative weight (%/°C) of (a) neat LDPE and with (b) NFC-pCot, (c) NFC-BSW, and (d) NFC-UBSW at reinforcing filler contents of 10 wt %. [Color figure can be viewed in the online issue, which is available at wileyonlinelibrary.com.]

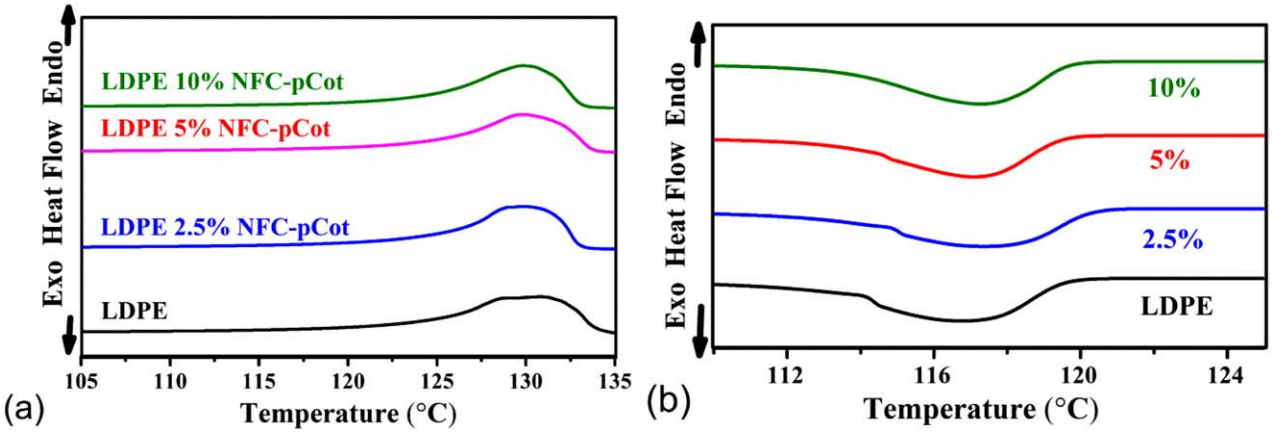

Figure 10. DSC thermograms of neat LDPE and with NFC-pCot at reinforcing filler contents of 2.5, 5, and 10 wt % (a) Heating thermogram of melting endotherm, (b) Cooling thermogram of crystallization exotherm. [Color figure can be viewed in the online issue, which is available at wileyonlinelibrary.com.]

(from hardwood)-reinforced maleic anhydride–modified PP nanocomposites.[25] The degree of crystallinity could be calculated using the heat of fusion/crystallization and eq. (2). Unlike the T_m and T_c, the degree of crystallinity (X_c%) increased upon addition of reinforcing agent probably due to a nucleating effect of cellulose nanofibers, and it is more pronounced using NFC-pCot.

Table IV. Thermal Characteristics of LDPE-Based Nanocomposites Obtained from DSC Analysis

Sample	T_m	ΔH_m	X_c%	T_c
LDPE	130.3 ± 0.02	175.9 ± 0.40	61.3 ± 0.02	117.0 ± 0.01
LDPE 2.5% NFC-pCot	129.7 ± 0	174.8 ± 0.26	62.4 ± 0.06	117.5 ± 0.01
LDPE 5% NFC-pCot	129.8 ± 0.03	180.4 ± 0.23	66.2 ± 0.05	117.5 ± 0.02
LDPE 10% NFC-pCot	130.1 ± 0.01	179.1 ± 0.04	69.3 ± 0.12	117.0 ± 0.01
LDPE 2.5% NFC-BSW	129.9 ± 0.01	181.1 ± 0.06	64.7 ± 0.02	117.3 ± 0.02
LDPE 5% NFC-BSW	131.1 ± 0.2	176.4 ± 0.11	64.0 ± 0.04	116.8 ± 0.1
LDPE 10% NFC-BSW	128.9 ± 0.01	162.1 ± 0.26	62.1 ± 0.07	117.8 ± 0
LDPE 2.5% NFC-UBSW	129.7 ± 0.04	176.4 ± 0.05	63.04 ± 0.02	117.4 ± 0
LDPE 5% NFC-UBSW	130.1 ± 0.2	174.6 ± 0.23	64.0 ± 0.3	117.8 ± 0.01
LDPE 10% NFC-UBSW	129.9 ± 0	169.8 ± 0.33	65.7 ± 0.2	117.4 ± 0

(T_m) melting temperature, (ΔH_m) enthalpy of fusion, (X_c%) degree of crystallinity, and (T_c) temperature of crystallization. $X_c = \Delta H_m / w.\Delta H_m^\circ$, where ΔH_m° (~287 Jg^{-1}) heat of fusion for 100% crystalline LDPE and w is the weight fraction of polymeric matrix in the composite.

Increasing the degree of crystallinity could partially improve the stiffness of LDPE nanocomposites. Incorporation of ramie cellulose whisker with LDPE also improved the degree of crystallinity of nanocomposites from 38% to 51% with filler percentage up to 15%.[12] Similar increased crystallinity of PLA was observed for the addition of NFC[21] and for PCL with sisal nanowhiskers.[23] In contrast, the X_c% of PCL nanocomposites modified with NFC from sisal fibers mechanically treated with a microfluidizer slightly remained constant.[24] Abdelmouleh and Yao also did not observe any improvement in degree of crystallinity of LDPE and HDPE upon addition of silane treated lignocellulosic fibers with average length of 2.5 mm and rice straw fibers, respectively.[26,27]

CONCLUSIONS

This research provides a comparative analysis in the use of microgrinding to fabricate NFC from pulverized cotton (derived from cotton T-shirts), bleached and unbleached softwood and outlines the use of these NFC materials in the mechanical reinforcement of a LPDE polymer matrix. Through the microfibrillation process, the size of the materials was successfully reduced to nanoscale diameters. NFC-pCot-filled nanocomposite films had higher modulus, tensile strength, and elongation to break than NFC-BSW and NFC-UBSW at all weight %. This may be due to the NFC-pCot having higher crystallinity, smaller NFC elements, and more uniform dispersion within the polymer matrix. The NFC in the composites caused the LDPE to have higher thermal stability within the experimental conditions used.

ACKNOWLEDGMENTS

The authors gratefully acknowledge financial support from Cotton Inc. (12–358). The cooperation of MeadWestvaco Company to process NFC-pCot is also greatly appreciated. We also thank Prof. Behnam Pourdeyhimi and the N.C. State Nonwovens Institute for providing LDPE polymer and NCRC characterization facilities. We would like to thank Dr. Hassan Sadeghifar (N.C. State) provided for assistance in freeze drying and extrusion processes.

REFERENCES

1. Missoum, K.; Belgacem, M. N.; Bras, J. *Materials* **2013**, *6*, 1745.
2. Eichhorn, S. J.; Dufresne, A.; Aranguren, M.; Marchovich, N. E.; Capadona, J. R.; Rowan, S. J.; Wedar, C.; Thielemans, W.; Roman, M.; Renneckar, S.; Gindl, W.; Veigel, S.; Keckes, J.; Yano, H.; Abe, K.; Nogi, M.; Nakagaito, A. N.; Mangalam, A.; Simonsen, J.; Benight, A. S.; Bismarck, A.; Berglund, L. A.; Peijs, T. *Mater. Sci.* **2010**, *45*, 1.
3. Spence, K. L.; Venditti, R. A.; Rojas, O. J; Habibi, Y.; Pawlak, J. J. *Cellulose* **2010**, *17*, 835.
4. Turbak, A. S. F.; Sandberg, K. *J. Appl. Polym. Sci.* **1983**, *37*, 815.
5. Lopez-Rubio, A.; Lagaron, J. M.; Ankerfors, M.; Lindström, T.; Nordqvist, D.; Mattozzi, A.; Hedenqvist, M. S. *Carbohydr. Polym.* **2007**, *68*, 718.
6. Tingaut, P.; Zimmermann, T.; Lopez-Suevos, F. *Biomacromolecules* **2010**, *11*, 454.
7. Spence, K. L.; Venditti, R. A.; Rojas, O. J; Habibi, Y.; Pawlak, J. J. *Cellulose* **2011**, *18*, 1097.
8. Orts, W. J.; Shey, J.; Imam, S. H.; Glenn, G. M.; Guttman, M. E.; Revol, J. F. *J. Polym. Environ.* **2005**, *13*, 301.
9. Farahbakhsh, N.; R. A. V.; Jur, J. S. *Cellulose* **2014**, *21*, 2743.
10. Agarwal, U. P.; Reiner, R. S.; Filpponen, I.; Isogai, A. Crystallinities of Nanocrystalline and Nanofibrillated Celluloses by FT-Raman Spectroscopy, in TAPPI International Conference on Nanotechnology for the Forest Product Industry; TAPPI: Helsniki, (**2010**).
11. Cheng, Q.; Wang, S. Q.; Rials, T. G.; Lee, S. H. *Cellulose* **2007**, *14*, 593.
12. de Menezes, A. J.; Siqueira, G.; Curvelo, A. A. S.; Dufresne, A. *Polymer* **2009**, *50*, 4552.
13. Zhang, J. J.; Rizvi, G. M.; Park, C. B. *Bioresources* **2011**, *6*, 4979.
14. Eyholzer, C.; Bordeanu, N.; Lopez-Suevos, F.; Rentsch, D.; Zimmermann, T.; Oksmann, K. *Cellulose* **2010**, *17*, 19.
15. Cheng, Q. Z.; Wang, S. Q.; Han, Q. Y. *J. Appl. Polym. Sci.* **2010**, *115*, 2756.
16. Spence, K. L.; Venditti, R. A.; Habibi, Y.; Rojas, O. J.; Pawlak, J. J. *Bioresource Technol.* **2010**, *101*, 5961.
17. Iwamoto, S.; Nakagaito, A. N.; Yano, H. *Appl. Phys. A-Mater* **2007**, *89*, 461.
18. Abe, K.; Yano, H. *Cellulose* **2009**, *16*, 1017.
19. Lu, J.; Wang, T.; Drzal, L. T. *Compos. Part A-Appl. S.* **2008**, *39*, 738.
20. Lu, J.; Askeland, P.; Drzal, L. T. *Polymer* **2008**, *49*, 1285.
21. Seydibeyoglu, M. O.; Oksman, K. *Compos. Sci. Technol.* **2008**, *68*, 908.
22. Trovatti, E.; Olivera, L.; Freire, C. S. R.; Silvestre, J. D.; Neto, C. P; Cruz, J. J. C.; Gandini, A. *Compos. Sci. Technol.* **2010**, *70*, 1148.
23. Kaushik, A.; Singh, M.; Verma, G. *Carobohydr. Polym.* **2010**, *82*, 337.
24. Siqueira, G.; Bras, J.; Dufresne, A. *Biomacromolecules* **2009**, *10*, 425.
25. Panaitescu, D. M.; Donescu, D.; Bercu, C.; Vulugu, D. M.; Iorga, M.; Ghiurea, M. *Polym. Eng. Sci.* **2007**, *47*, 1228.
26. Abdelmouleh, M.; Boufis, S.; Belgacem, M. N.; Dufresne, A. *Composites Science and Technology* **2007**, *67*, 1627.
27. Yao, F.; Wu, Q.; Lei, Y.; Xu, Y. *Industrial Crops and Products* **2008**, *28*, 63.